Polar accumulation of pyoverdin facilitates rapid exit from stationary phase

Clara Moreno-Fenoll[a,b], **Maxime Ardré**[a], **and Paul B. Rainey**[a,b]

[a]Laboratory of Biophysics and Evolution, CBI, ESPCI Paris, Université PSL, CNRS, 75005 Paris, France; [b]Department of Microbial Population Biology, Max Planck Institute for Evolutionary Biology, August-Thienemann Str. 2, 24306 Plön, Germany

This manuscript was compiled on June 16, 2023

Pyoverdin is a water-soluble metal-chelator synthesized by members of the genus *Pseudomonas* and used for the acquisition of insoluble ferric iron. Although freely diffusible in aqueous environments, preferential dissemination of pyoverdin among adjacent cells, fine-tuning of intracellular siderophore concentrations, and fitness advantages to pyoverdin-producing versus nonproducing cells, indicate control of location and release. Here, using time-lapse fluorescence microscopy to track single cells in growing microcolonies of *Pseudomonas fluorescens* SBW25, we show accumulation of pyoverdin at cell poles. Accumulation occurs on cessation of cell growth, is achieved by cross-feeding in pyoverdin-nonproducing mutants and is reversible. Moreover, accumulation coincides with localization of a fluorescent periplasmic reporter, suggesting that pyoverdin accumulation is part of the general cellular response to starvation. Compatible with this conclusion is absence of non-accumulating phenoytpes in a range of pyoverdin mutants. Analysis of the performance of pyoverdin-producing and nonproducing cells under conditions promoting polar accumulation shows an advantage to pyoverdin on resumption of growth after stress. Examination of polar accumulation of pyoverdin in a multispecies community and in a range of laboratory and natural species of *Pseudomonas*, including *P. aeruginosa* PAO1 and *P. putida* KT2440, confirms that the phenotype is characteristic of *Pseudomonas*.

cytoplasmic shrinkage | periplasmic space | stationary phase | ecological relevance | growth resumption

DRAFT

Extracellular secreted products perform important functions in microbial communities. They provide structure and protection (1), enable coordinated action (2) (3), and facilitate acquisition of recalcitrant nutrients, such as polymers that are too large to be internalized (4), or are otherwise unavailable. An example of the latter is pyoverdin.

Pyoverdin is a naturally fluorescent iron-scavenging chelator (sideropohore) produced by members of the genus *Pseudomonas* (5). Iron is an essential micronutrient that exists in an insoluble state (ferric) in aerobic environments (6). In response to intracellular iron scarcity, pyoverdin biosynthesis begins in the cytoplasm via nonribosomal peptide synthesis and undergoes maturation in the periplasm (7). After secretion, it binds Fe^{3+} with high affinity (Ka = 10^{32} M^{-1} for PVDI produced by *P. aeruginosa* PAO1 (8)). Once bound to ferric iron the ferripyoverdin complex loses its fluorescent properties, but is recognized by a specific receptor (FpvA) and imported back into the periplasm, where iron is extracted. The pyoverdin molecule is then recycled and can undergo further cycles of export and import (9).

The eco-physiology of pyoverdin is complex and poorly understood. Complexity arises at the physiological level from the interplay between the redox status of iron (with effects on bio-availability), and cellular demands that are balanced against potentially lethal toxic effects. For example, in aerobic environments, where bio-availability of iron is low and cellular demand high, cells risk harm from hydroxyl radicals liberated via the Fenton reaction. One role of pyoverdin is as protectant against intracellular oxidative stress (10). But pyoverdin has roles beyond iron-specific chemistry: pyoverdin chelates other metals, including magnesium, zinc and gallium, with roles in homeostasis and detoxification of these and other metals (11). Challenges arise from the need to understand the ecological relevance of numerous diverse forms of pyoverdin (12), the plethora of ferri-pyoverdin receptors (13, 14), and the various roles of pyoverdin in shaping interactions with eukaryotic hosts (15–17).

Because pyoverdin is a soluble extracellular product, it is widely assumed to be equally available to all members of a community (18–20). However, recent work shows that its distribution is subject to cell-level control. In one study pyoverdin producers retained an environment-dependent fitness advantage in conditions where invasion by nonproducers was expected (21). In light of these experimental results, the possibility of personalization was raised (21). Other studies have further supported this notion. For example, in growing microcolonies, pyoverdin diffuses primarily between adjacent cells, reducing loss into the environment (22). Furthermore, *Pseudomonas aeruginosa* cells tune periplasmic concentrations of pyoverdin in order to protect against oxidative stress (10).

Here we use time-lapse fluorescence microscopy to study the relationship between *P. fluorescens* SBW25 cells and pyoverdin. Recognizing the importance of spatial structure and contributions therefrom to µm-scale features of microbial as-

Significance Statement

Bacteria secrete extracellular products that enable nutrients to be obtained from the environment. A secreted product of significance to medicine, agriculture and biotechnology is the iron-chelating siderophore, pyoverdin, produced by members of the genus *Pseudomonas*. By analyzing the behavior of single cells we show that on cessation of cell division, pyoverdin accumulates at cell poles and does so in periplasmic space created by cytoplasmic shrinkage. The behavior is ecologically relevant: on encountering growth-permissive conditions, cells liberate pyoverdin and exit stationary phase with minimal delay. Our study connects a general biophysical stress response to a molecule of physiological and ecological importance.

PBR, CMF and MA designed research. CMF performed research. CMF and MA analyzed data. PBR, CMF and MA wrote the paper.

Authors declare no competing interests.

[2]To whom correspondence should be addressed. E-mail: clara.moreno-fenoll@espci.psl.eu

semblages (23–26), cells were grown on thin layers of agarose set on top of microscope slides. In actively dividing cells, naturally fluorescent apo-pyoverdin is evenly distributed in the periplasm, however, on cessation of growth we observed pyoverdin to accumulation at cell poles. This surprising discovery motivated quantitative analysis, revealing the process of polar accumulation to be dynamic, reversible, and ecologically relevant.

Results

Polar accumulation of pyoverdin. *P. fluorescens* SBW25 (hereafter SBW25) is a model bacterium (27) known to produce pyoverdin (28) and other secreted products (29, 30). In a previous study Zhang & Rainey (21) provided evidence of pyoverdin personalization that was inferred following contrasting outcomes of fitness assays performed under different conditions. We reproduced these assays, but rather than examining frequencies of producers and nonproducers by plating, aliquotes were observed by fluorescence microscopy. In casamino acids medium (CAA), the medium where an unexpected advantage for pyoverdin producers had been described, cells exhibited internal pyoverdin accumulation more evident at the pole where fluorescent foci appeared (Fig. 1A). This initial observation provoked further analysis.

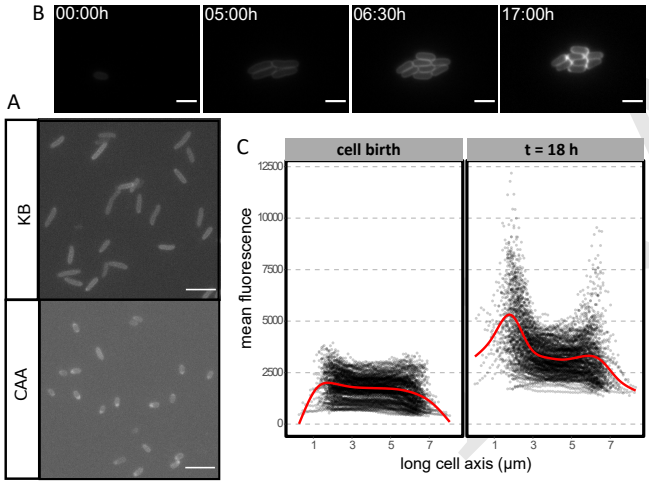

Fig. 1. Polar accumulation of pyoverdin in *P. fluorescens* SBW25 at the cell pole. A) Images from experiments described in (21) where fitness assays of pyoverdin producing SBW25 and a nonproducing *pvdS* defective mutant yield contrasting results depending on the culture medium. In both cases the environment is unstructured and ancestral SBW25 producer cells are rare, inoculated at 1%. A fitness advantage to nonproducing cells in KB was previously reported, but the reverse in CAA (21). In KB (top) pyoverdin nonproducing cells rarely showed evidence of accumulation of pyoverdin, whereas (bottom) this was common in CAA-cultured cells where accumulation is visible at the pole. Images were obtained from $3\,\mu l$ samples of these experiments imaged under fluorescent light (excitation 390 nm / emission 475 nm) to visualize pyoverdin. All scale bars correspond to $10\,\mu m$. B) Fluorescence (390/475 nm) time-lapse images of a growing microcolony of SBW25 on an agarose pad of succinate minimal medium (SMM). Images represent selected time points including, respectively: the initial inoculum, exponential growth, end of exponential growth, and end of time-lapse acquisition (18 h total) C) Mean fluorescence intensity along the long axis of cells in a growing microcolony, when the last generation of cells is born (left) and at the end of acquistion (t = 18 h, right). Black dotted lines represent the fluorescence profile of individual cells, the red line represents a smoothed mean of all cells. Between 0 h and 18 h accumulation of pyoverdin is evident, especially at the pole.

To accurately characterize subcellular patterns of pyoverdin, time-lapse fluorescence images of ancestral SBW25 were obtained in defined succinate minimal medium (SMM), where succinate acts both as carbon source and weak iron chelator. During exponential phase and early stationary phase, SBW25 cells showed a phenotype typical of fluorescent *Pseudomonas* with pyoverdin being homogeneously distributed in the periplasm. In late stationary phase fluorescent pyoverdin foci appeared at the cell pole, indicating accumulation of the siderophore. Polarization of pyoverdin was evident by qualitative observation (Fig. 1B) and was verified after image analysis and segmentation by superposing fluorescence profiles at different time points (Fig. 1C).

By examining cell division throughout the time-lapse series it was possible to explore the dynamic accumulation of pyoverdin. The corresponding frequency of polarized cells (Fig. 2A) was tracked by classifying segmented cells automatically as "accumulated" and "non-accumulated" using a machine learning algorithm (Supplementary Materials and Methods). After inoculation onto microscope slides, cells undergo a period of acclimation without division. No polar accumulation of pyoverdin was observed during this phase. As division begins, age of cells in microcolonies decreases until it reaches a minimum that marks exponential phase. Pyoverdin continued to be evenly distributed. Note that the small frequency of cells identified as “accumulation” in the plot falls within the range of classification error. Finally, the population enters stationary phase and cells continue ageing without division. Accumulation of pyoverdin at cell poles increased within the first few hours and was evident in a majority of cells by 18h (duplicate experiments are given Fig. S1).

While the time-averaged state of microcolonies exposes population-level dynamics of polarization – namely, that accumulation happens in stationary phase – it obscures the behavior of individual cells. To specifically analyze single bacteria, cells were grouped according to division status over three generations: F0 for initial inoculum (cells where birth could not be identified but division was observed), F1 for cells in exponential phase (born from the division of F0 cells and later underwent division) and F2 for the daughter cells of F1 that entered stationary phase and remained constant for the final hours of the experiment. Growth measurements from F1 cells, and pyoverdin accumulation measurements from F2 cells, corroborate – despite some variability in the onset of accumulation – that accumulation of pyoverdin is incompatible with active cell division. Cells either elongate, or accumulate fluorescence (pyoverdin) at the cell pole. This result holds for both old and new poles (Fig. 2B). Curiously, pyoverdin accumulates preferentially at the new pole, but not exclusively, and sometimes distinct foci are present at both (Fig. S2)

Stationary phase marks cessation of cell division due to nutrient depletion. On an agarose pad, entry into stationary phase is highly variable, with access of cells to nutrients and oxygen depending on position and proximity to neighbouring cells. To study pyoverdin accumulation under controlled conditions cells were exposed to two stressors that abruptly arrest cell division, but by different mechanisms: 1, an iron chelating agent (2,2'-dipyridil (DP)) and; 2, a protein synthesis-disrupting antibiotic (tetracycline)(Fig. S4A). Both stressors induced accumulation at the pole (Fig. 2C).

Precisely because polarization appears when cells are starved and/or stressed, processes associated with cell death,

such as cell wall damage, are potential elicitors. We thus asked whether pyoverdin accumulation was connected to cell viability. Bacteria were treated with DP, which reliably induced polarization (Fig. 2C) and then transferred to a fresh agarose pad. Time-lapse imaging revealed that polar accumulation of pyoverdin is reversible and that depolarization precedes exit from lag phase (Fig. 2D). Cells that accumulated pyoverdin at the pole consistently re-established a homogeneous distribution within the first few hours after inoculation, with elongation and division resuming at a later time point (Fig. S4B). Note that both the initial frequency of polarized cells and the time to depolarization were counted from the start of image acquisition. During the previous experimental manipulation, some individuals might have altered their polarization status. Despite this, the trend is clear, with depolarization occurring before resumption of growth. Polarization is thus not a consequence of cell death but rather a reversible, dynamic process tied to arrest of cell division.

Mechanism of pyoverdin accumulation. Pyoverdin polarization is clearly connected to the physiological state of cells, but how this is achieved is unclear. A recent study showed that the cytoplasm of *E.coli* shrinks on starvation leading to enlargement of periplasmic space at cell poles (31). We hypothesized that this might also occur in *P.fluorescens* cells, with the space created by shrinkage allowing accumulation of pyoverdin. To this end, a red fluorescent protein (mScarlet) was translationally fused to a peptide signal from *dsbA* thus enabling targeting of mScarlet to the periplasm (See SI). Having confirmed periplasmic localization, cells were grown on agarose pads and the distribution of mScarlet was tracked by microscopy. At inoculation mScarlet was homogeneously distributed as observed for pyoverdin. However, on entry into stationary phase, the fluorescent marker accumulated at cell poles (Fig. 3A). As with pyoverdin, mScarlet accumulation was biased toward new poles (Fig. 3B). Unlike pyoverdin, mScarlet showed no evidence of secretion to the external medium (Fig. S7)

While overlap in patterns of pyoverdin and periplasm-targeted mScarlet accumulation points towards the fact that pyoverdin polarization is coupled to general cellular phenomena, possibilities remain for the involvement of genetic determinants of pyoverdin biosynthesis, regulation and transport. To test this hypothesis, patterns of pyoverdin accumulation were monitored in a range of mutants. However, we first asked whether polar accumulation of pyoverdin is a consequence of defective periplasmic maturation (32): SBW25 producer and nonproducer types (the latter with an mCherry fluorescent marker) were co-cultured. Pyoverdin was localized in non-producing cells (Fig. 3D.1) demonstrating that accumulated pyoverdin is functional, since any siderophore internalized by the nonproducing mutant necessarily comes from the external medium after export by SBW25. Polarization thus involves pyoverdin that is actively used among cells of the population.

Next, recognizing that mature pyoverdin interacts with membrane proteins via OpmQ (33, 34), *opmQ* was deleted and the pattern of pyoverdin accumulation determined. SBW25 Δ*opmQ* showed no change in capacity to accumulate pyoverdin at cell poles (Fig. 3D.2), however, the mutant showed increased intracellular levels of pyoverdin though secretion was not abolished (Fig. S5A)(11).

Pyoverdin synthesis is subject to positive feedback control via the pyoverdin receptor FpvA making this protein a candidate for involvement in pyoverdin accumulation (7). Production of pyoverdin by SBW25Δ*fpvA* was significantly reduced compared to ancestral SBW25 (Fig. S5B), however, where pyoverdin was visible, it was polarized as in ancestral SBW25 (Fig. 3D.3).

While the genes involved in extraction of ferric iron and translocation into the cytoplasm have not been characterized in *P. fluorescens*, a recent study in *P. aeruginosa* suggests potential candidates for polarization including a siderophore-binding periplasmic protein (9). Deletion of the homologs of these genes in SBW25 PFLU_2048, PFLU_2041, and PFLU_2043 did not disrupt accumulation of pyoverdin (Fig. S6). Thus, neither aggregation of pyoverdin at trafficking points across the periplasm, nor accumulation via the ferripyoverdin complex recycling system, are involved in polarization.

Additional possibilities for polar accumulation are via connections to extracellular polymer synthesis and cell morphology. SBW25 secretes cellulose when constructing bacterial mats at the air-liquid interface (30, 35), which could trap pyoverdin at the perimeter of cells. However, pyoverdin localization was not altered in SBW25 Δ*wsp*Δ*aws*Δ*mws* (36) that is unable to produce cellulose (Fig. 3D.4). Finally, the rod-cell-shape characteristic of *Pseudomonas* was considered a possible contributory factor. To test this, pyoverdin accumulation was observed in a spherical Δ*mreB* mutant (37). Despite the aberrant cell shape, this mutant displayed fluorescence foci of pyoverdin after extended culture (Fig. 3D.5).

Fitness effects. Polar accumulation of pyoverdin is linked to cell physiology, but is unperturbed by known genetic determinants of pyoverdin biosynthesis, regulation, or transport. This leads to the possibility that pyoverdin accumulation under conditions of cellular stress is an accidental consequence of the biophysics of cell biology and lacks ecological relevance. The alternate hypothesis is one of ecological relevance: a plausible explanation being that release of accumulated pyoverdin allows cells to reduce the time required to exit stationary phase.

An ideal test would be an experiment in which time to resumption of growth of an ancestral type that accumulates pyoverdin is compared to a mutant unable to accumulate pyoverdin, under conditions where pyoverdin accumulation both occurs, and doesn't occur. If accumulation of pyoverdin confers a fitness advantage, then ancestral types are expected to resume growth more rapidly than non-accumulating mutants, but only after cells have first experienced conditions that promote accumulation of pyoverdin.

Unfortunately, as evident above, no such pyoverdin-accumulating mutant exists, nonetheless, progress is possible via an experiment that exploits the fact that a PvdS mutant cannot accumulate pyoverdin because it is unable to produce it. To this end, SBW25 and a PvdS mutant (SBW25 *pvdSG229A*(D77N) (21) (hereafter termed Pvd$^-$) were grown separately in SMM for sufficient time to ensure cells entered stationary phase (24 h). A sample of cells from both populations was then transferred to independent SMM agarose pads and the time to first cell division determined. While a slight delay in median time for resumption of growth was observed in Pvd$^-$ compared to SBW25 the distribution of data points shows significant overlap. The findings were not affected by transfer of cells from overnight SMM culture to agarose pads additionally supplemented with excess iron (Fig. 4A, left).

DRAFT

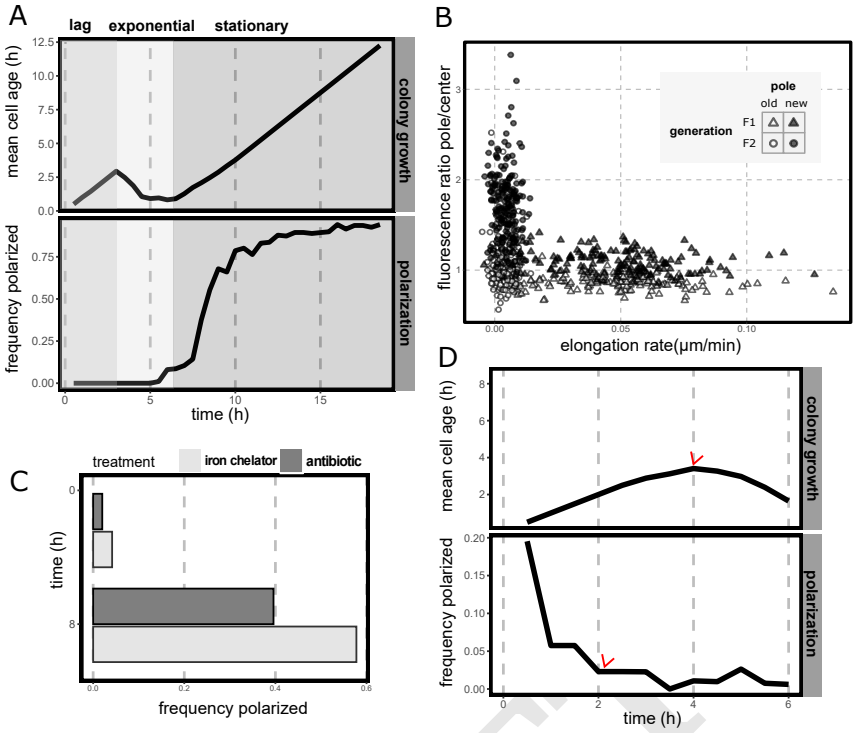

Fig. 2. Polar accumulation is a reversible phenotype associated with arrest of cell division. A) Polarization in different growth stages of a microcolony. Mean age of the cells in a growing microcolony of SBW25 (black line, top) and the corresponding frequency of polarized cells for each time point (black line, bottom). Colored panels represent the growth stages of the microcolony, from left to right: lag phase (generation F0), exponential phase (generation F1), and stationary phase (generation F2). N= 35, 159, 187 respectively. In all cases data has been filtered to exclude cells with segmentation errors or other artifacts that preclude proper analysis. Note that as microcolonies begin to form in exponential phase and cells are no longer isolated, overlap between adjacent cells creates regions of high fluorescence that could lead to classification errors. Nevertheless, visual inspection reveals that cells remain in a homogeneous state during exponential growth, with polarization onset being clearly associated to stationary phase. B) Elongation rate and accumulation of fluorescence at the cell pole of individual cells in a growing microcolony. Data extracted from A). Markers represent individual cells in different growth phases of the colony (F1, exponential, triangle markers; F2, stationary, circle markers) and the old (white markers) and new (black markers) cell pole. Elongation rate is represented by the average over the lifetime of a cell. Accumulation of fluorescence at the pole is represented by the maximum ratio over the lifetime of a cell of the sum of the pixels in the pole region and central region of a cell. These regions are defined by segmenting the cell and dividing it in 3 portions over the long axis, where the external 1/3 represent each pole and the remaining 1/3 represents the center. C) Polarization in response to chemical stresses related and unrelated to iron metabolism. Bars represent the frequency of polarized cells at the start of treatment and after 8h of treatment with either $100\,\mu g \cdot ml^{-1}$ 2,2'-dipyridil (DP) (light bars) or $5\,\mu g \cdot ml^{-1}$ tetracycline (dark bars). No cell division was observed during treatment. N = 99 (t=0h), 94 (t = 8h) and N = 94 (t = 0h), 79 (t = 8h) for DP and tetracyline treatments respectively. D) Depolarization and subsequent growth of cells pre-treated with an iron chelator. Plot represents colony growth and polarization as in A). Cells were treated with $100\,\mu g \cdot ml^{-1}$ DP during 4h, washed and inoculated on a fresh SMM agarose pad. Data corresponds to five technical replicates i.e., five positions on the agarose pad. Red arrows indicate the time point where the colony overall starts growing (top) and where the majority of the cells are depolarized (bottom). Total initial number of cells N=87.

This indicates that even the Pvd$^-$ mutant was not deficient in iron despite having entered stationary phase.

Results were significantly different when the 24 h preculture period in SMM included a final 4 h period during which populations of both SBW25 and Pvd$^-$ experienced iron-stress arising from supplementation of SMM with the iron chelating agent DP. As shown above, a 4 h treatment with DP not only caused cessation of growth, but also triggered polar accumulation of pyoverdin. The effect of this treatment was to greatly extend the time to resumption of growth in the non-pyoverdin-accumulating mutant. This difference was eliminated when cells, having experienced iron-deprivation, were provided with excess iron on SMM agarose pads (Fig. 4A, right). These results demonstrate a fitness advantage to accumulation of pyoverdin that stems from a reduction in time to exit stationary phase.

This conclusion is further supported by the results of an additional experiment in which SBW25 and the Pvd$^-$ mutant were grown as previously, treated with DP and then mixed in a 1:1 ratio and then transferred to a fresh SMM agarose pad. Measurement of the time to resume growth showed little difference among the competing genotypes (Fig. 4B). This is consistent with the expectation that SBW25 releases accumulated pyoverdin into the (fresh) medium to the benefit of both producer and non-producer alike. Notable though is the fact that producer cells reap greatest benefit. When nonproducers are instead inoculated in the presence of rare ancestor cells ($\sim 1\%$) their lag time again increases significantly, supporting the conclusion that newly released pyoverdin underpins the faster division of producers (Fig. S8). Furthermore, the amount of pyoverdin accumulated during starvation seems to be sufficient to support at least twice as many cells, as the lag time of SBW25 producer cells was not affected by the presence of nonproducers.

Pyoverdin accumulation in community context. We further tested pyoverdin polarization in conditions closer to the natural milieu of SBW25, where species inter-dependencies are common and resources invariably limiting. To implement a minimal bacterial community, SBW25 was co-cultured with

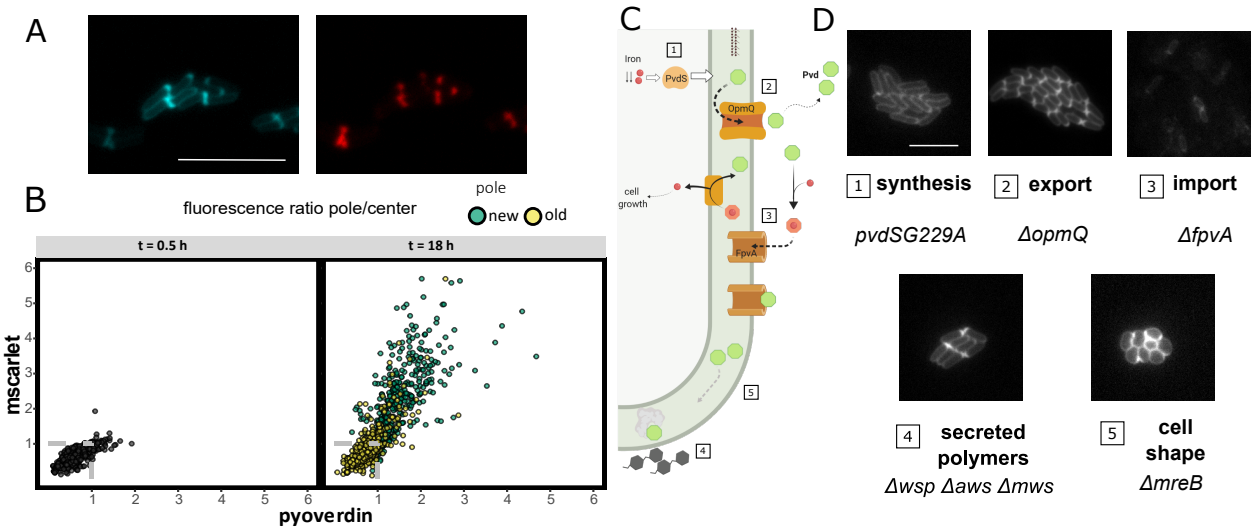

Fig. 3. Untangling the mechanism of polarization. A) A recent study (31) showed that upon starvation the cytoplasm of *E. coli* cells shrinks creating extra space in the periplasm at cell poles (typically the new pole). To determine whether a similar phenomenon occurs in *P. fluorescens* SBW25 a red fluorescent mScarlet protein (excitation 550 nm/ emission 605nm) was translationally fused to the localization signal peptide of DsbA, a periplasmic protein. The image obtained at t = 18 h shows co-localization of pyoverdin fluorescence (left, blue) and mScarlet (right, red, scale bar represents $10\,\mu m$). B) Quantitative analysis of time-resolved images at 30 min and 18 h. Cells were segmented and intensity of fluorescence was measured along the long axis. Fluorescence at the poles was contrasted with the signal produced at center of each cell; this was done for both pyoverdin (x-axis) and mScarlet (y-axis). Dots represent the intensity ratio for both fluorescent molecules. For measurements at 18 h the values for both the new pole (green dots) and old pole (yellow dots) are represented. Polar information is not available for freshly inoculated cells. The gray dashed line highlights the values where the center of the cell and the poles are not substantially different, *i.e.*, the ratio is close to 1. Deviation from this value indicates polar accumulation of the molecules. C) Cartoon depicting a simplified version of the pyoverdin pathway in which candidate genes for polarization are shown. [1] Pyoverdin (Pvd) synthesis starts in the periplasm in response to iron scarcity mediated by the transcription factor PvdS. Pyoverdin is then secreted to the bacterial periplasm, where it matures and becomes fluorescent. [2] Periplasmic pyoverdin is exported into the external medium by a complex that includes the transporter OpmQ. There, it chelates insoluble iron (Fe^{3+}). [3] Ferripyoverdin complexes (no longer fluorescent) are then imported back into the periplasm after binding to the receptor FpvA. This receptor is known to also bind free pyoverdin (7). In the periplasm, iron is extracted and pyoverdin is again recycled into the external medium by OpmQ. Polarization might also be determined by genes unrelated to the pyoverdin pathway: [4] SBW25 is known to secrete polymers such as cellulose that might trap pyoverdin (30). [5] Pyoverdin could accumulate at the cell poles due to the rod shape of SBW25. D) Mutants associated to the main processes depicted in A) and their phenotype with regards to pyoverdin polarization. Mutants were grown on an agarose pad as described and fluorescence images displaying pyoverdin were taken after 16 h. The pyoverdin nonproducing mutant *pvdSG229A*(D77N) was co-inoculated with SBW25 to enable access of the mutant to pyoverdin. This mutant was tagged with a red fluorescent protein to aid identification.

a cellulose-degrading *Bacillus* isolated from a compost heap on minimal medium with cellulose as sole carbon source (38). Because SBW25 is unable to degrade cellulose, it must rely on the *Bacillus* species to obtain carbon for growth. These two co-cultured strains were imaged to assess polarization status. Pyoverdin was readily observed to be polarized (Fig. 5A). Pyoverdin accumulation at the cell pole is thus likely to be part of the natural phenotypic repertoire of SBW25, and given that in natural environments bacteria likely find themselves in or close to stationary phase most of the time, polar accumulation of pyoverdin might be the normal state.

Polarization across *Pseudomonas*. Since pyoverdins of many different types are produced by a wide range of species belonging to the genus *Pseudomonas*, investigating subcellular distribution in related strains stands to provide an evolutionary context for polar accumulation. We selected 11 strains belonging to the genus *Pseudomonas*, comprising both common laboratory strains (such as *P. aeruginosa* PAO1, in which pyoverdin has been extensively studied) and natural isolates from different European locations. The ability of these strains to polarize pyoverdin was classified qualitatively, that is, presence or absence of polarized cells (Fig. 5B). All tested strains accumulated pyoverdin at cell poles in conditions similar to those described here for SBW25. Interestingly, different strains accumulated pyoverdin with treatments of varying stringency. In some cases extended culture in SMM was sufficient to observe the phenotype (e.g., *P. putida* KT2440). In others, amendment with an iron chelator was necessary to observe the effect (e.g., *P. aureofaciens* U149), at the same dosage that induced polarization in SBW25, and in the specific case of *P. aeruginosa* PAO1, very high doses of DP were required. This range of responses could reflect the secretion of secondary siderophores by some strains (12) or differences in the regulation of pyoverdin production (20), and suggest that polarization is an ecologically relevant trait that varies depending on the evolutionary history of each lineage.

Discussion

Previous work showing that the population-level distribution of pyoverdin changes depending on nutrient status (21), contact with neighboring cells (22), and environmental stress (10) motivated our investigation. With focus on *P. fluorescens* SBW25, and using time-resolved microscopy, we have shown that pyoverdin transiently accumulates at cell poles, that localization is a reversible process associated with arrest of cell division, and is affected by factors such as entry into stationary phase and deprivation of specific nutrients (Fig. 2). Particularly significant is demonstration that accumulation of pyoverdin has ecological relevance (Fig. 4).

Investigations at the level of individual cells have proved essential for linking behavior of cells to the dynamics of populations (24, 25). For example, Gore et al (2009) (39) showed that

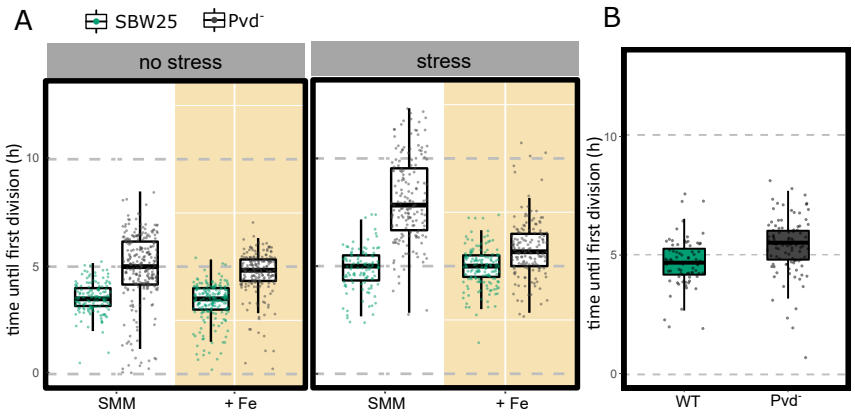

Fig. 4. Pyoverdin polarization facilitates recovery of growth after stress. A) Time until first division (lag time) of SBW25 (green) and pyoverdin non-accumulating mutant *pvdSG229A*(D77N), termed Pvd$^-$ (gray) under different treatments and conditions. Prior to inoculation cells were either grown in the usual culture medium SMM (no stress on left panel) or treated with DP for 4h (stress on right panel). Cells were then inoculated on a fresh agarose pad, supplemented with 0.45 mM $Fe_2[SO_4]_3$ where labeled "+ Fe" (yellow background) or in unmodified SMM medium (labeled "SMM", white background). Dots represent individual cell values, box plots represent the associated distribution (median, 25th and 75th percentiles) N = 145, 261, 199, 193, 111, 168, 156, 156 respectively from left to right. B) Time until first division of SBW25 (green) and Pvd$^-$ mutants co-inoculated in a fresh agarose pad after separate stress treatment (4h in DP). Pvd$^-$ mutants were labeled with a red fluorescent protein to allow identification of individual cells on the pad. Dots and box plots as in A). N = 175 total cells.

the cellular location of invertase responsible for degradation of sucrose in *Saccharomyces cerevisiae* creates diffusion gradients of degradation products that deliver benefit to producing cells, despite cost to producers of synthesizing the enzyme (39). Similarly, the siderophore enterochelin (a catecholate secreted by *E. coli* and other *Enterobacteriaceae*) can remain associated with the outer membrane under conditions of low cell density, delivering preferential benefit to enterochelin-producing cells (40).

Also arising from cell-level investigations has come recognition of dynamic localization of proteins at cell poles (41). In some instances proteins oscillate between poles (42), whereas others accumulate via formation of nuclear occlusions in the cytoplasm (43). In the context of pyoverdin, complexes termed "siderosomes" localize enzymes for synthesis of pyoverdin at old cell poles during exponential growth by association of the cytoplasmic membrane with L-ornithine N5-oxygenase (encoded by *pvdA*) (44, 45).

While we most often observed accumulation of pyoverdin at new cell poles, it was also evident at old poles, and on occasion it was found at both poles. Lack of location specificity hinted at a connection to more general biophysical aspects of cell biology. Interestingly, a recent study of *E. coli* under starvation conditions showed polar accumulation of fluorescent markers, including mCherry (31). Accumulation was connected to shrinkage of the cytoplasm, with shrinkage creating an expansion of space in the polar region of the periplasm. It thus seemed plausible that pyoverdin accumulation in stationary phase may be a consequence of nonspecific cellular behavior under growth arrest. Such a possibility was bolstered by the fact that a PvdS mutant deficient in synthesis of pyoverdin (and thus lacking siderosomes) nonetheless accumulated pyoverdin, that deletion of genetic determinants of uptake and recycling had no observable effects on accumulation, and that pyoverdin accumulation also occurred at discrete locations in spherical Δ*mreB* cells (Fig. 3D.5).

To investigate the hypothesis that pyoverdin accumulation is connected to cytoplasmic shrinkage, red fluorescent mScarlet was translationally fused to the localization signal peptide of DsbA. As cells entered stationary phase accumulation of the fluorescent marker protein was observed at cell poles in a manner analogous to that observed for pyoverdin. In fact, single images captured using filters specific for the reporter protein and pyoverdin showed an almost perfect overlap (3A,B). This leads to the conclusion that polar accumulation of pyoverdin is part of a general cellular response to starvation. Thus observations made in *E. coli* with a chimeric reporter (31) appear to hold for SBW25, but with our observations connecting cytoplasmic shrinkage to accumulation of a biologically relevant molecule. Additionally we demonstrate that accumulation delivers beneficial effects on fitness.

Data in Fig. 4A show that cells with localized pyoverdin resume growth more rapidly compared to non-accumulating cells. A time-to-first cell division advantage was not evident when growth-arrested cells were transferred to iron-replete conditions. This demonstrates that liberation of the stock of pyoverdin accumulated during growth cessation speeds the time to growth resumption after growth arrest, presumably through provision of available iron to growing cells. 4B.

Of additional interest is evidence from cell-level observations that rare pyoverdin producers are largely unaffected by the presence of Pvd$^-$ mutants (Fig. S8). Such mutants have often been referred to as "cheats" and thus expected to negatively impact the fitness of pyoverdin producers (so called "cooperators"). Lack of detrimental impact is further evidence that pyoverdin production preferentially benefits producer cells and is indicative of preferential benefit to pyoverdin producing cells. This finding further calls into question the fit between social evolution theory and production of extracellular products by microbes (20, 21). It also gels with work showing that populations of siderophore-producing *Pseudomonas* can be grown in the presence of an excess of nonproducing mutants without a significant reduction in overall yield (46).

Recent work suggests important physiological differences between acute (and unexpected) interruptions of cell division, and gradual growth arrest that determines entry into stationary phase (47). In the former case, sudden arrest induces a disrupted state that results in large variability in cell-level duration of lag phase. In the latter case, cells implement genetic programs that buffer the effects of impending starvation creating cohesive population-level responses (47). The seemingly adaptive nature of pyoverdin accumulation under stress is reminiscent of – and perhaps even connected to – the capacity of SBW25 to enter a semi-quiescent capsulated state upon starvation. During starvation, SBW25 cells produce an excess of ribosomes that allow rapid exit from stationary phase once

DRAFT

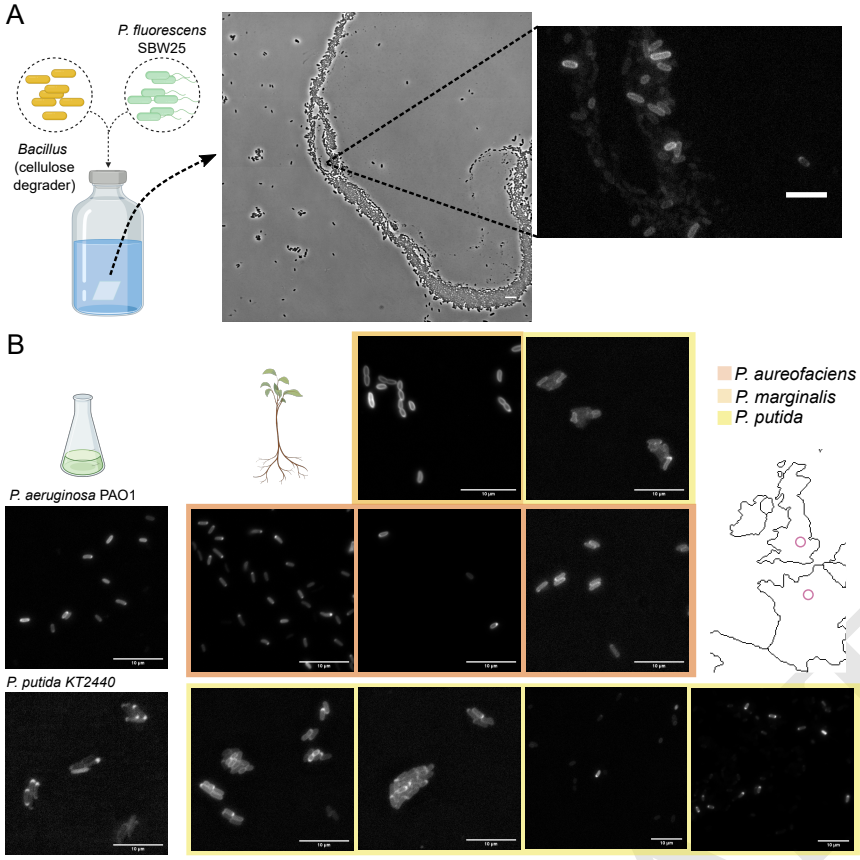

Fig. 5. Polar accumulation of pyoverdin is evident in SBW25 in a multispecies community and is a common phenotype in related species of the genus *Pseudomonas*. A) Polarized SBW25 cells in a multispecies community with interdependencies. SBW25 and a cellulose-degrading *Bacillus* strain isolated from a compost heap in Paris, France (38) were co-cultured in glass vials with minimal medium and cellulose paper as the only carbon source. The community was periodically sampled to assess the polarization state of SBW25. A representative image obtained after 28 days of growth is displayed, where both strains are visible (left, phase contrast image) and in a magnified region where pyoverdin distribution in SBW25 is visualized (right, fluorescence image). B) Qualitative accumulation assessment in species of *Pseudomonas* other than SBW25. A collection of laboratory (left) and natural (right) strains were tested for accumulation reported by polarization. Accumulation reported by polarization in commonly used laboratory strains: *P. aeruginosa* PAO1 tested in SMM agarose pad with $1000\,\mu g \cdot ml^{-1}$ DP for 7:30 h; *P. putida* KT2440 tested in SMM agarose pad for 24h. Polarization test in natural isolates, left to right and top to bottom: U106 (liquid KB medium for 24 h); U177 (SMM agarose pad for 24 h); U149 (liquid SMM with DP $100\,\mu g \cdot ml^{-1}$ for 24 h); U180 (liquid SMM with DP $100\,\mu g \cdot ml^{-1}$ for 24 h); U181 (SMM agarose pad for 16 h); T24 V1a (SMM agarose pad for 24 h); T24 V9b (SMM agarose pad for 24 h); T24 H1b (SMM agarose pad for 24 h); T24 H9b (liquid SMM for 24 h). Natural isolates were collected in Oxford, UK (56) (first and second row) and in Paris, France (38) (Bottom row). Locations are roughly marked with a pink circle on the map. The frame colors represent the identified *Pseudomonas* species.

growth-permissive conditions are encountered. Cells unable to provision ribosomes are quickly out-competed by those that do (48). It is possible that localization of pyoverdin, followed by fast release under growth permissive conditions, has evolved as a strategy precisely because it maximizes competitive performance upon resumption of growth. Rapid resumption of growth is likely to deliver significant fitness benefits in environments punctuated by periods of nutrient abundance and scarcity.

Mounting evidence indicates that pyoverdin – in its many variant forms (12) – has multiple impacts on composition and function of microbial communities (49–54). The fact that pyoverdin is accumulated and localized under growth limiting conditions in a diverse range of *Pseudomonas*, combined with evidence of the same behavior in SBW25 cells grown for weeks under nutrient restrictive conditions with reliance on cellulose degrading *Bacillus* (Fig. 5), suggests that polarization has relevance to conditions beyond those experienced by cells in standard, nutritionally-rich, exponential-phase, laboratory culture.

Given that pyoverdin accumulation appears connected to cytoplasmic shrinkage, it seems reasonable to assume that other molecules may similarly accumulate in the periplasm in response to division arrest signals, which both change size and shape of cellular compartments. Indeed, accumulation of products related to nutrient stress is one possible function of the bacterial periplasm, with roles analogous to vacuoles in eukaryotes (55).

Materials and Methods

Strains, culture media, and reagents. Ancestral *Pseudomonas fluorescens* SBW25 originally isolated on beet roots at the University of Oxford farm (Wytham, Oxford, U.K.) (27) and a collection of relevant mutants were used: the pyoverdin nonproducer *pvdsG229A*(D77N) named Pvd⁻ in the main text (construction described in (21)), the corresponding strain with mCherry fluorescence tagging under IPTG induction, Δ*mreB*, PBR716 (Δ*wsp*Δ*aws*Δ*mws*, described in (36)). Pyoverdin import and export defective mutants Δ*PFLU3979* (OpmQ) and Δ*PFLU2545* (FpvA) were created by two-step allelic exchange (57). The periplasm reporter strain was created by fusing the red fluorescent protein mScarlet to the signal peptide of periplasmic protein, DsbA (see Supplementary Methods). A neutrally marked SBW25 strain (58) was used to replicate the fitness assays from (21). *Escherichia coli* DH5α λ_{pir} and pRK2013 were used for cloning. *Bacillus* 002.IH from Steven Quistad's compost heap collection (38) was used for the community experiment. For the phylogenetic comparison, an assortment of species of the genus *Pseudomonas* were selected from the lab collection. Most experiments were performed in succinate minimal medium (SMM, described in (22)). Overnight cultures were done in Luria-Bertani (LB) broth. Replication of fitness assays was performed in CAA and KB media as described in the original work (21). Community experiment was done in M9 minimal medium with cellulose as the only carbon source (Whatman). Where indicated media was supplemented with 2,2'-dipyridil (Sigma), tetracycline (Duchefa, France), $Fe_2[SO_4]_3$(III) (Sigma), IPTG (Melford). For strain construction tetracycline, nitrofurantoin (Sigma), X-gal (Melford), D-cycloserine (Duchefa) were used.

Agarose pad. To prepare the agarose pad, 220 µl of agarose (Melford) dissolved in SMM (2% w/v) were poured onto a microscope slide fitted with a sticky frame (Gene Frame, Fisher Scientific), pressed with a clean slide and allowed to dry for $\sim$ 2 min. A small $\sim$ 3 mm

DRAFT

section of the pad and frame was cut across the slide to provide air for the growing cells. 1.5 µl of washed culture was inoculated on the agarose pad and sealed with a coverslip.

Microscopy. Inoculated agarose pads were monitored by taking snapshots every 30 min for a typical total time of 18h using the microscope Axio Observer Z1 (Zeiss, Germany). Cells were imaged under phase contrast (exposure: 100 ms) and fluorescence corresponding to Pvd using the fluorescence Source X-Cite 120 LED and the following filters: 390/40 BrightLine HC, Beamsplitter T 425 LPXR, 475/50 BrightLine HC (exposure: 30 ms, 12 % intensity for pyoverdin fluorescence and 100 ms 20 % intensity for red fluorescence). Images were taken with 63x and optovar 1.6x magnification.

Image analysis. Image processing was performed using the image analysis software Image J. Segmentation and analysis was performed using the package for Matlab SuperSegger from the Wiggins Lab (59). Further analysis and data visualization was carried out with the programming software R. After segmentation cells were sorted by polarization status using a classificator obtained with the Statistics and Machine Learning Toolbox for Matlab (More details in SI).

Community experiment. SBW25 and *Bacillus* 002.IH (from (38)) were grown on 20 ml M9 minimal medium and cellulose as the only carbon source (1 cm x 1 cm cellulose paper). After overnight growth cultures were washed and co-inoculated into 20 ml of M9 medium with cellulose paper in a 60 ml vial. These vials were incubated at room temperature with unscrewed caps to allow air exchange, and periodically sampled for imaging.

Phylogenetic comparison. A collection of laboratory and natural strains belonging to the genus *Pseudomonas* were subjected to a binary qualitative polarization test, i.e. the test was considered positive if polarized cells were observed under fluorescence microscopy in conditions similar to SBW25 but no dynamics were assessed. Commonly used laboratory strains *P. aeruginosa* PAO1 and *P. putida* KT2440 were tested. Natural isolates belong to collections from two different locations. Paris, France (38): T24 V1a, T24 V9b, T24 H1b, T24H9b; all classified as *P. putida*. Oxford, UK (56): *P. marginalis* U106, *P. putida* U177, *P.aureofaciens* U149, U180, and U181.

ACKNOWLEDGMENTS. We thank Dave Rogers for assistance with construction of mutants and valuable discussion. We thank Steven D. Quistad and Xue-Xian Zhang for supplying *Pseudomonas* isolates. PBR acknowledges generous core support from the Max Planck Society.

1. HC Flemming, et al., Biofilms: an emergent form of bacterial life. *Nat. Rev. Microbiol.* **14**, 563–575 (2016).
2. JW Newman, RV Floyd, JL Fothergill, The contribution of Pseudomonas aeruginosa virulence factors and host factors in the establishment of urinary tract infections. *FEMS Microbiol. Lett.* **364** (2017).
3. M Diard, et al., Stabilization of cooperative virulence by the expression of an avirulent phenotype. *Nature* **494**, 353–356 (2013).
4. NR Gilkes, DG Kilburn, RC Miller, RA Warren, Bacterial cellulases. *Bioresour. Technol.* **36**, 21–35 (1991).
5. JM Meyer, MA Abdallah, The fluorescent pigment of Pseudomonas fluorescens: Biosynthesis, purification and physicochemical properties. *J. Gen. Microbiol.* **107** (1978).
6. JB Neilands, Iron absorption and transport in microorganisms. *Annu. review nutrition* **1** (1981).
7. MT Ringel, T Brüser, The biosynthesis of pyoverdines. *Microb. cell* **5**, 424–437 (2018).
8. AM Albrecht-Gary, S Blanc, N Rochel, AZ Ocaktan, MA Abdallah, Bacterial iron transport: coordination properties of pyoverdin PaA, a peptidic siderophore of Pseudomonas aeruginosa. *Inorg. Chem.* **33** (1994).
9. A Bonneau, B Roche, IJ Schalk, Iron acquisition in Pseudomonas aeruginosa by the siderophore pyoverdine: an intricate interacting network including periplasmic and membrane proteins. *Sci. Reports* **10**, 120 (2020).
10. Z Jin, et al., Conditional privatization of a public siderophore enables Pseudomonas aeruginosa to resist cheater invasion. *Nat. Commun.* **9**, 1383 (2018).
11. IJ Schalk, L Guillon, Pyoverdine biosynthesis and secretion in Pseudomonas aeruginosa : implications for metal homeostasis. *Environ. Microbiol.* **15**, 1661–1673 (2013).
12. P Cornelis, S Matthijs, Diversity of siderophore-mediated iron uptake systems in fluorescent pseudomonads: Not only pyoverdines. *Environ. Microbiol.* **4**, 787–798 (2002).
13. EE Smith, EH Sims, DH Spencer, R Kaul, MV Olson, Evidence for diversifying selection at the pyoverdine locus of Pseudomonas aeruginosa. *J. Bacteriol.* **187**, 2138–2147 (2005).
14. J Bodilis, et al., Distribution and evolution of ferripyoverdine receptors in Pseudomonas aeruginosa. *Environ. Microbiol.* **11**, 2123–2135 (2009).
15. F Minandri, et al., Role of iron uptake systems in pseudomonas aeruginosa virulence and airway infection. *Infect. Immun.* **84**, 2324–2335 (2016).
16. F Taguchi, et al., The siderophore pyoverdine of Pseudomonas syringae pv. tabaci 6605 is an intrinsic virulence factor in host tobacco infection. *J. Bacteriol.* **192**, 117–126 (2010).
17. P Trapet, et al., The Pseudomonas fluorescens siderophore pyoverdine weakens Arabidopsis thaliana defense in favor of growth in iron-deficient conditions. *Plant physiology* **171**, 675–93 (2016).
18. SA West, SP Diggle, A Buckling, A Gardner, AS Griffin, The social lives of microbes. *Annu. Rev. Ecol. Evol. Syst.* **38**, 53–77 (2007).
19. A Buckling, et al., Siderophore-mediated cooperation and virulence in Pseudomonas aeruginosa. *FEMS Microbiol. Ecol.* **62**, 135–141 (2007).
20. PB Rainey, N Desprat, WW Driscoll, XX Zhang, Microbes are not bound by sociobiology: Response to Kümmerli and Ross-Gillespie (2013). *Evolution* **68**, 3344–3355 (2014).
21. XX Zhang, PB Rainey, Exploring the sociobiology of pyoverdin-producing Pseudomonas. *Evolution* **67**, 3161–3174 (2013).
22. T Julou, et al., Cell-cell contacts confine public goods diffusion inside Pseudomonas aeruginosa clonal microcolonies. *Proc. Natl. Acad. Sci. United States Am.* **110**, 12577–82 (2013).
23. SK Hansen, PB Rainey, JA Haagensen, S Molin, Evolution of species interactions in a biofilm community. *Nature* **445** (2007).
24. OX Cordero, MS Datta, Microbial interactions and community assembly at microscales. *Curr. Opin. Microbiol.* pp. 227–234 (2016).
25. AD Co, S van Vliet, DJ Kiviet, S Schlegel, M Ackermann, Short-range interactions govern the dynamics and functions of microbial communities. *Nat. Ecol. Evol.* **4**, 366–375 (2020).
26. R Hartmann, et al., Emergence of three-dimensional order and structure in growing biofilms. *Nat. Phys.* **15**, 251–256 (2019).
27. MW Silby, et al., Genomic and genetic analyses of diversity and plant interactions of Pseudomonas fluorescens. *Genome Biol.* **10**, R51 (2009).
28. CD Moon, et al., Genomic, genetic and structural analysis of pyoverdine-mediated iron acquisition in the plant growth-promoting bacterium Pseudomonas fluorescens SBW25. *BMC Microbiol.* **8**, 7 (2008).
29. K Hammerschmidt, CJ Rose, B Kerr, PB Rainey, Life cycles, fitness decoupling and the evolution of multicellularity. *Nature* **515**, 75–9 (2014).
30. AJ Spiers, SG Kahn, J Bohannon, M Travisano, PB Rainey, Adaptive divergence in experimental populations of Pseudomonas fluorescens. I. Genetic and phenotypic bases of wrinkly spreader fitness. *Genetics* pp. 33–46 (2002).
31. H Shi, et al., Starvation induces shrinkage of the bacterial cytoplasm. *Proc. Natl. Acad. Sci.* **118**, e2104686118 (2021).
32. E Yeterian, et al., Synthesis of the siderophore pyoverdine in Pseudomonas aeruginosa involves a periplasmic maturation. *Amino Acids* **38**, 1447–1459 (2010).
33. E Yeterian, LW Martin, IL Lamont, IJ Schalk, An efflux pump is required for siderophore recycling by Pseudomonas aeruginosa. *Environ. Microbiol. Reports* **2**, 412–418 (2009).
34. IJ Schalk, et al., Iron-free pyoverdin binds to its outer membrane receptor FpvA in Pseudomonas aeruginosa: a new mechanism for membrane iron transport. *Mol. Microbiol.* **39**, 351–361 (2001).
35. M Ardré, D Dufour, PB Rainey, Causes and biophysical consequences of cellulose production by pseudomonas fluorescens sbw25 at the air-liquid interface. *J. Bacteriol.* **201** (2019).
36. MJ McDonald, SM Gehrig, PL Meintjes, XX Zhang, PB Rainey, Adaptive divergence in experimental populations of Pseudomonas fluorescens. IV. Genetic constraints guide evolutionary trajectories in a parallel adaptive radiation. *Genetics* **183**, 1041–53 (2009).
37. P Yulo, et al., Experimental Evolution of Cell Shape in Bacteria. *bioRxiv* p. 263681 (2018).
38. SD Quistad, G Doulcier, PB Rainey, Experimental manipulation of selfish genetic elements links genes to microbial community function. *Philos. Transactions Royal Soc. B: Biol. Sci.* **375**, 20190681 (2020).
39. J Gore, H Youk, A van Oudenaarden, Snowdrift game dynamics and facultative cheating in yeast. *Nature* **459**, 253–6 (2009).
40. RL Scholz, EP Greenberg, Sociality in Escherichia coli: Enterochelin is a private good at low cell density and can be shared at high cell density. *J. Bacteriol.* **197**, 2122–2128 (2015).
41. L Shapiro, HH McAdams, R Losick, Generating and exploiting polarity in bacteria. *Science* **298**, 1942–1946 (2002).
42. DM Raskin, PAJ De Boer, Rapid pole-to-pole oscillation of a protein required for directing division to the middle of Escherichia coli MATERIALS AND METHODS. *Cell Biol.* **96**, 4971–4976 (1999).
43. G Laloux, C Jacobs-Wagner, How do bacteria localize proteins to the cell pole? *J. Cell Sci.* **127** (2013).
44. L Guillon, M El Mecherki, S Altenburger, PL Graumann, IJ Schalk, High cellular organization of pyoverdine biosynthesis in Pseudomonas aeruginosa: clustering of PvdA at the old cell pole. *Environ. Microbiol.* **14**, 1982–1994 (2012).
45. V Gasser, L Guillon, O Cunrath, I Schalk, Cellular organization of siderophore biosynthesis in Pseudomonas aeruginosa: Evidence for siderosomes. *J. Inorg. Biochem.* **148**, 27–34 (2015).
46. Ö Özkaya, R Balbontín, I Gordo, KB Xavier, Cheating on cheaters stabilizes cooperation in Pseudomonas aeruginosa. *Curr. Biol.* **28**, 2070–2080.e6 (2018).
47. Y Kaplan, et al., Observation of universal ageing dynamics in antibiotic persistence. *Nature* **600**, 290–294 (2021).
48. P Remigi, et al., Ribosome provisioning activates a bistable switch coupled to fast exit from stationary phase. *Mol. Biol. Evol.* **36**, 1056–1070 (2019).
49. JW Kloepper, J Leongt, M Teintzet, MN Schroth, Enhanced plant growth by siderophores produced by plant growth-promoting rhizobacteria. *Nature* **286**, 885–886 (1980).
50. D Haas, G Défago, Biological control of soil-borne pathogens by fluorescent pseudomonads. *Nat. Rev. Microbiol.* **3**, 307–319 (2005).
51. P Stilwell, C Lowe, A Buckling, The effect of cheats on siderophore diversity in Pseudomonas aeruginosa. *J. Evol. Biol.* **31**, 1330–1339 (2018).
52. P Mirleau, et al., Fitness in soil and rhizosphere of Pseudomonas fluorescens C7R12 com-

DRAFT

pared with a C7R12 mutant affected in pyoverdine synthesis and uptake. *FEMS Microbiol. Ecol.* **34**, 35–44 (2000).
53. E Banin, ML Vasil, EP Greenberg, Iron and Pseudomonas aeruginosa biofilm formation. *Proc. Natl. Acad. Sci.* **102**, 11076–11081 (2005).
54. G Sass, et al., Studies of Pseudomonas aeruginosa mutants indicate pyoverdine as the central factor in inhibition of Aspergillus fumigatus biofilm. *J. Bacteriol.* **200** (2018).
55. AM Brauer, H Shi, PA Levin, KC Huang, Physiological and regulatory convergence between osmotic and nutrient stress responses in microbes. *Curr. Opin. Cell Biol.* **81**, 102170 (2023).
56. XX Zhang, et al., Genotypic and phenotypic analyses reveal distinct population structures and ecotypes for sugar beet-associated Pseudomonas in Oxford and Auckland. *Ecol. Evol.* **10**, 5963–5975 (2020).
57. XX Zhang, PB Rainey, Genetic analysis of the histidine utilization (hut) genes in Pseudomonas fluorescens SBW25. *Genetics* **176**, 2165–76 (2007).
58. XX Zhang, PB Rainey, Construction and validation of a neutrally-marked strain of Pseudomonas fluorescens SBW25. *J. Microbiol. Methods* **71**, 78–81 (2007).
59. S Stylianidou, C Brennan, SB Nissen, NJ Kuwada, PA Wiggins, SuperSegger: robust image segmentation, analysis and lineage tracking of bacterial cells. *Mol. Microbiol.* **102**, 690–700 (2016).

DRAFT